

REPORT DOCUMENTATION PAGE				Form Approved OMB No. 0704-0188	
Public reporting burden for this collection of information is estimated to average 1 hour per response, including the time for reviewing instructions, searching data sources, gathering and maintaining the data needed, and completing and reviewing the collection of information. Send comments regarding this burden estimate or any other aspect of this collection of information, including suggestions for reducing this burden to Washington Headquarters Service, Directorate for Information Operations and Reports, 1215 Jefferson Davis Highway, Suite 1204, Arlington, VA 22202-4302, and to the Office of Management and Budget, Paperwork Reduction Project (0704-0188), Washington, DC 20503. PLEASE DO NOT RETURN YOUR FORM TO THE ABOVE ADDRESS.					
1. REPORT DATE (DD-MM-YYYY) 12/17/2014		2. REPORT TYPE Final Report		3. DATES COVERED (From - To) 11/01/2010—8/31/2014	
4. TITLE AND SUBTITLE Modeling Statistics of Fish Patchiness and Predicting Associated Influence on Statistics of Acoustic Echoes				5a. CONTRACT NUMBERS	
				5b. GRANT NUMBER N00014-11-1-0147	
				5c. PROGRAM ELEMENT NUMBER	
6. AUTHOR(S) Dr. Timothy K. Stanton Daniel Grunbaum Thomas Weber				5d. PROJECT NUMBER	
				5e. TASK NUMBER	
				5f. WORK UNIT NUMBER	
7. PERFORMING ORGANIZATION NAME(S) AND ADDRESS(ES) Applied Ocean Physics & Engineering Department Woods Hole Oceanographic Institution 98 Water Street, MS #11 Woods Hole, MA 02543				8. PERFORMING ORGANIZATION REPORT NUMBER	
9. SPONSORING/MONITORING AGENCY NAME(S) AND ADDRESS(ES)				10. SPONSORING/MONITORING ACRONYM(S)	
				11. SPONSORING/MONITORING AGENCY REPORT NUMBER	
12. DISTRIBUTION/AVAILABILITY STATEMENT Approved for public release; distribution is unlimited					
13. SUPPLEMENTARY NOTES					
14. ABSTRACT See Attached Report					
15. SUBJECT TERMS Fish patchiness and acoustic echoes					
16. SECURITY CLASSIFICATION OF:			17. LIMITATION OF ABSTRACT UL	18. NUMBER OF PAGES 21	19a. NAME OF RESPONSIBLE PERSON Dr. Timothy K. Stanton
a. REPORT UL	b. ABSTRACT UL	c. THIS PAGE UL			19 b. TELEPHONE NUMBER (Include area code) 508-289-2757

2014 1223035

Modeling Statistics of Fish Patchiness and Predicting Associated Influence on Statistics of Acoustic Echoes

Final Report December, 2014

Timothy K. Stanton
Applied Ocean Physics and Engineering Department
Woods Hole Oceanographic Institution
Bigelow 201, MS #11
Woods Hole, MA 02543
phone: (508) 289-2757 fax: (508) 457-2194 email: tstanton@whoi.edu

Daniel Grunbaum
School of Oceanography
University of Washington
Seattle, WA 98195-7940
email: grunbaum@ocean.washintgon.edu

Thomas C. Weber
Center for Coastal and Ocean Mapping
Jere A. Chase Ocean Engineering Laboratory
University of New Hampshire
Durham, NH 03824
email: weber@ccom.unh.edu

Award Number: N00014-11-1-0147

<http://www.whoi.edu/people/tstanton>

LONG-TERM GOALS

To accurately describe the statistics of acoustic echoes due to the presence of fish, especially in the case of a long-range active sonar. Toward this goal, fundamental advances in the understanding of fish behavior, especially in aggregations, will be made under conditions relevant to the echo statistics problem.

OBJECTIVES

To develop new models of behavior of fish aggregations, including the fission/fusion process, and to describe the echo statistics associated with the random fish behavior using existing formulations of echo statistics.

APPROACH

Several interrelated components of research are conducted in parallel and in a synergistic way: One important component of the research is the development of new advanced models of fish behavior

inspired by, and grounded by, 3-D images of fish aggregations. These images are derived by multi-beam acoustic systems. Key parameters to be observed and modeled are the rate of fission/fusion of the aggregations. Concurrent with the modeling of fish behavior, observed statistics of fish aggregations, as they become available, will be incorporated into an existing general formulation for echo statistics, as well as being used to parameterize previously published, and the newly developed, behavior models. The results of these latter efforts will, in turn, help to drive further development of the fish behavior model. Some of the fish aggregation data comes from NOAA/Fisheries, as they conduct these measurements as part of their routine surveys. The Stanton/Weber/Grunbaum group participated in planning their experiments which yielded data that reveal key aspects of fish behavior and, in turn, contributes to the modeling.

Stanton oversaw the entire project as well as worked on predicting echo statistics from fish in an ocean waveguide and applied existing fish behavior models to existing 3-D images of fish aggregations. Weber analyzed images of fish aggregations that he and NOAA/Fisheries have recently collected for parameterization and incorporation into new theoretical models. Grunbaum developed the new fish behavior models and parameterized them with data analyzed in this project. The work also involved informal collaborations with Chris Wilson of NOAA Alaska Fisheries and Ben Jones of NPS.

WORK COMPLETED

Major milestones were reached in all components of the project--- a new model for fish behavior was developed, optimized for numerical efficiency, and used to make predictions with empirical parameters; 3-D images of fish schools were measured with multi-beam sonars and quantified in terms of important aspects of fish dynamics; and predictions were made of echo statistics of a long-range sonar in a realistic ocean waveguide with fish present. Results from this project have been presented at scientific conferences and are summarized in four scientific papers (two published and two more submitted to refereed scientific journals.) In addition, some of the fundamental scientific results were transitioned in a concurrent applied program (ONR HiFAST FNC program) to both NAVSEA and NAVAIR sonar trainers.

The scientific results are given in detail in the following sections.

1. New model for fish school behavior

A novel approach was created in this project towards understanding fission, fusion, and migration of social groups (fish, in this case) by assuming a high level of sensory and cognitive function by interacting individuals. We published the following paper summarizing the results: Grunbaum (2012). Simulations based on this model show all of these behavioral aspects, as illustrated in the time series of fish distribution in Figure 1.

Nearly all current models of social interaction are "zone models" which assume that characteristics of animal groups such as schools, swarms and flocks arise from individuals' immediate responses to the relative positions and velocities of a small number of nearest neighbors. While there is little question that position- and velocity-dependent responses are crucial to social grouping, current zone models commonly predict that large groups (that is, groups in which individuals in different parts of a group must interact indirectly through many individuals between them) should be fragile and therefore rare or transient. However, natural groups are frequently large and stable. In other settings, natural populations that are sparse or distributed in numerous small groups nonetheless maintain common orientation

across groups. In most current zone models, directionality can be maintained only by frequent encounters between individuals and groups, and so is unlikely in sparse populations at reasonable levels of behavioral and physical random forcing.

The new model assumes an additional cognitive layer in fish schooling behavior, in which encounters with neighbors are used as input data on which to base statistical estimates of the density and movement characteristics of the local population. The key idea is that each individual is continuously updating its understanding of the intent of its neighbors, and basing its own decision-making on this understanding. Thus, social individuals can glean information even when the instantaneous position and velocity of neighbors are quite different from overall movement patterns, or when neighbors are so sparse that encounters with them are rare.

The above line of reasoning suggests a new hybrid model that combines agent-based "Lagrangian" movement rules with a "Eulerian" distribution of population density and flux, together with local distributions of orientation angle. This hybrid approach has multiple advantages from the perspective of understanding acoustic signatures of fish in real-world settings. One is computational tractability: Agent-based models of social grouping are inherently N^2 computations, where N is the number of individuals. (Specifying maximum interaction distances can enable subdivision of the habitat into non-interacting parts, but computational requirements remain large for dense groups.) The hybrid model executes parallel simulations, in which the estimates of local population characteristics evolve as partial differential equations, and the individuals respond to estimates as autonomous agents. Hence, there is no N^2 calculation required. Another advantage of our hybrid approach is that the statistical distributions calculated during social simulations (population density, orientation angles, etc.) are directly relevant to estimates of acoustic signatures.

The hybrid modeling assumes a Bayesian framework for local estimation of population movement. For example, for estimates of local density, we assume each individual maintains a Bayesian updating scheme for determining the expected value and uncertainty associated with the Poisson distribution of neighbors. In a standard updating scheme, appropriate for statistically stationary neighbor distributions, the uncertainty decreases monotonically with ongoing sampling. In application to schooling, in which populations move and therefore are not statistically stationary, we discount the predictive value of old information. Hence, an individual's uncertainty about local density and direction fluctuates downwards when informative samples occur frequently and upwards when such samples are rare.

2. Parameterizing and optimizing new model for fish school behavior

This work followed the above development (Section 1) of the new fish schooling model and focused on estimating parameters of the new model using individual-level and population-level fish schooling data. The individual-level data are 10-minute-long 3-dimensional-trajectory sequences of all individuals within small schooling and milling aggregations in the laboratory. The population-level data were collected in field surveys of Alaska pollock being analyzed by Weber and Stanton as described below in Section 3. The model and its application to schooling analysis involve a relatively large number of parameters, which must be constrained and optimized with respect to the available data. Therefore, much of the effort also involved building computational and statistical machinery to execute this optimization. Both the number of parameters and the relatively high computational demands of large-scale spatially-explicit schooling models make effectiveness and efficiency key to successful parameter-fitting. The principal modeling accomplishments, specific to parameterizing and optimizing, are summarized:

(a) We reanalyzed individual-level fish trajectory data to comprehensively characterize individual positions and movements within groups and to quantify neighbor-neighbor turning and acceleration responses. We developed new computational machinery for parameter-fitting behavioral models to our individual-level fish trajectory data. We conducted large-scale numerical optimization to obtain best-fitting behavioral response zones for short-memory cases. We have also extended our analysis to long-memory cases. We conducted simulations using the best-fit behaviors to assess the degree to which they reflect the observed behaviors from which they were extracted (Fig. 2).

(b) We developed model computer code to embed observed fish trajectories into the new cognitive schooling model. This enables us to conduct simulations in which modeled fish respond to actual observed fish behavior. This also enables us to assess model behaviors by replacing one or more members of a real fish aggregation with a simulated counterpart, and quantifying the degree to which position, movement and neighbor-neighbor responses are statistically consistent with the true behavior.

(c) We developed model computer code to identify and characterize schools in the output of the cognitive schooling model (Fig. 3). Identification of schools is based largely on mathematical morphology analysis techniques for “segmentation” of features in images. Densities and edge characteristics of groups are used to delineate them from surrounding non-group distributions. This analytical machinery is a key tool in constraining model parameters to field surveys of fish schools that quantify distributions of group size, shape and separation distance.

(d) We developed computational infrastructure to extract cognitive behavior and other parameters from the NOAA Alaska Fisheries Science Center acoustic/trawl walleye pollock survey data. The central challenge in parameter estimation from data of this type is that data have incomplete spatial coverage and, at any given spatial position, are irregular in time. A consequence is that, within a set of repeated surveys, each acoustic transect reflects an unknown fraction of fish that were previously detected, that moved into the survey area since the last transect, or that left the survey area since the last transit.

Our approach to estimating parameters utilizes iterated simulations of behavioral models, maximizing statistical similarities between predicted and observed data where observations are available. The gist of this approach is that a model provides a means to accumulate information between intermittent and probably sparse data. The combination of data and movement mechanisms embedded in the equations enable the model to “learn” as much as possible about the state of the system. A necessary element in this maximization is as unbiased as possible a “null” population distribution for areas in which no observation data are available.

An example of this approach is given in Fig. 4 which shows estimates for the walleye pollock survey data using an advection-diffusion process as the underlying movement mechanism for fish populations. The analysis goes through the entire sequence of recent surveys, and determines the advection velocity and diffusion that yield the best matches between model and data (according to one of a number of statistical metrics, the figure reflects a correlation metric). In these data, the best-fit advection velocity for fish signals likely is dominated by the ambient current velocity. The diffusion coefficient reflects movement and fission/fusion of fish schools, possibly with contributions from other sources. With an estimate of the current velocity, we can remove water movement from the geo-referenced survey data to quantify how the fish are moving relative to the water in which they are immersed, reflecting the true school movement dynamics. There has also been work to implement this approach in more sophisticated behavioral models.

(e) Because cognitive schooling models have not been developed previous to this project, statistical methods for estimating cognitive behavioral parameters do not yet exist. To develop statistical tools for inferring these parameters, we considered a simpler spatial memory/cognition problem, which is the odor source location problem, applicable to many engineering and environmental problems of interest to the Navy. We had access to trajectories of male moths finding a pheromone-emitting female; our goal was to quantify the mate-seeking behavior of these male moths in a cognitive behavioral framework. This is a simpler parameter estimation problem because ways in which the geometry of plumes transported by turbulent environmental flows might be statistically summarized are known from fluid physics.

Using the moth dataset, we developed new biomimetic cognition-based algorithms for odor source location, and mapped out strategies for estimating parameters of models of spatial memory and cognition (Fig 5). We assumed that cognitive parameters were structured so as to estimate and respond to plume geometry in the most efficient way. The guidance to parameterizing behavioral parameters provided by this assumption was central to obtaining parameter estimates that explain large fractions of variance in observed movements. This work is described in a manuscript in collaboration with a chemosensory ecologist and was submitted to the Journal of Movement Ecology (Grunbaum and Willis, 2014). As with fish schooling, this is an entirely new approach to assessing this biological phenomenon, which will be stimulating and useful to a wide range of future investigations.

3. Extracting fish-behavior parameters from high resolution images of fish aggregations derived from acoustic multibeam data

Overview

Multibeam data analysis has focused mostly on data collected in the Eastern Bering Sea (EBS) during both 2010 and 2012. These data were collected using a Simrad ME70 multibeam echosounder as part of the NOAA Alaska Fisheries Science Center (NOAA-AFSC) acoustic/trawl walleye pollock surveys. Through use of sequential pings from the 2-D multibeam data, 3-D images of fish schools could be made (Figs. 6-8).

Data collections from both years represent multiple (approximately 9) week survey efforts aimed at broad-scale stock assessments in the EBS, and ME70 data have been made available to this project courtesy of Chris Wilson (NOAA-AFSC). Most of the data were collected along widely spaced (~40 km) transects, and for the purposes of this research are considered to represent a 'snapshot' of the pollock aggregations present in the EBS. During the 2012 data collection effort, NOAA-AFSC also conducted repeat transects at our request and with our guidance on two occasions. This resulted in ~1-nmi-long transects that were repeated every 10-15 minutes, with 24 transects on the first occasion and 14 transects on the second occasion. Analysis of the 2010 data focused on population level statistics. Analysis of the 2012 data concerned studying rates of schooling fission and fusion. These latter data were analyzed to extract metrics describing morphological changes in the fish aggregations that can be used to tune or ground-truth behavioral models. Metrics of particular interest include the size-dependent group speed and bounds on the rate at which aggregations appear to split (a 'fission' event) or recombine (a 'fusion' event).

ME70 data representing 8 days of survey effort in July 2010 were analyzed to form clusters of volumetric backscatter representing mid-water pollock aggregations (Figure 9). These data cover a

region extending from 176°W to 179.5°W and 58°N to 62.5°N. Mid-water trawls (N = 43) conducted in this region caught 98% pollock by weight. The ME70 data were processed to

- a. remove potential seabed returns and sidelobe contamination
- b. remove data below a threshold of $S_v = -60$ dB (independent of beam angle)
- c. remove spatially isolated targets that are considered ‘speckle’ noise
- d. cluster, and uniquely label, data that are within 25 m of each other horizontally and 5 m of each other vertically
- e. extract metrics describing each cluster including the cluster volume, V , maximum vertical extent, H , and maximum horizontal extent, L .

Statistics of fish school size—population level

49,650 clusters of fish were extracted for the 8 day period. Histograms of their effective size, $V^{1/3}$, vertical extent, and horizontal extent are shown in Figure 10. Also shown are best fits of the data to the models of Anderson [1981] and Niwa [2003], in a similar fashion to Stanton et al [submitted]. Neglecting issues that may arise from the ME70 finite field of view and range/angle-dependent resolution, the data suggest that the pollock aggregations have a high aspect ratio: the mode of the horizontal extent is approximately 6 times greater than the mode for the maximum vertical extent. The data can be fitted quite closely to the Anderson model, which assumed disk-like aggregations of fish and modeled the diameter of schools.

Statistics of fish school size—selected fish types

An important caveat in the population statistics shown in Figure 10 is that the data represent aggregations of both juveniles and adults, nighttime and daytime behaviors, other environmental covariates, and possible ‘contamination’ from other species. To examine this issue further, we have extracted population statistics from the 2012 repeat transects. The first set of repeat transects targeted small, dense fish aggregations (“cherry balls”) that were fully contained within the ME70 field of view. The second set of repeat transects targeted dense aggregations that could be acoustically mapped, but which likely extended outside of the field of view. For the first set of repeat transects (Figure 11), the fish aggregations observed on consecutive passes appeared to be uncorrelated, and were largely constrained to dense aggregations at water depths less than 80 m with a large, widely-spaced aggregation of targets below 80 m. The second set of repeat transects exhibited dense aggregations of fish throughout the water column, with a quasi-continuous distribution of fish below 80 m water depth and relatively well-separated aggregations in the upper portion of the water column (Figure 12). These data were processed similarly to the 2010 ME70 data, except that rather than cluster the data based on an *a priori* assumption about horizontal and vertical ‘linking’ distances, the data were contoured based on volume scattering strength. Aggregation metrics were subsequently calculated at the contour level representing a fish density 100x less than the peak density. This approach made it possible to treat discrete and quasi-continuous aggregations using the same methodology. The distribution of the effective school horizontal radius is shown in Figure 13 for the 1st set of repeat passes (‘subset 1’), and for the second set of repeat passes for fish observed in the upper 80 m of water (‘subset 2, upper 80 m’), below 80 m (‘subset 2, below 80 m’), and for a 10 m thick layer between 90-100 m (‘subset 2, 90-100 m’). Each distribution appears quite similar and, like the larger population of aggregations analyzed from the 2010 data, fit a power-law distribution of approximately L^{-3} for the larger aggregation sizes.

Fission/fusion dynamics

The repeat-transect data collected in 2012 were further analyzed to extract metrics describing morphological changes in the fish aggregations that can be used to tune or ground-truth behavioral models. Metrics of particular interest include the size-dependent group speed and bounds on the rate at which aggregations appear to split (a ‘fission’ event) or recombine (a ‘fusion’ event).

An example showing six passes (approximately 1:05 hours) over an aggregation of fish is shown in Figure 14 (upper panel). The dynamics of splitting and recombining of the aggregations are illustrated in the lower panel of Fig. 14. During the first two passes (A and B), the aggregations have approximately the same volume and volumetric scattering strength. The aggregation then splits into two subgroups over the subsequent two passes (C1/C2 and D1/D2). The split-aggregation then appears to recombine between the fourth and fifth passes, and remains mostly together on a sixth pass. During these passes, the group (or subgroup) volumes vary between $12,000 \text{ m}^3$ (C2) and $55,000 \text{ m}^3$ (F) and have speeds ranging from 0.9 cm/s (B to C2) and 6.8 cm/s (D1 to E). The scattering strength measurements suggest that there are $O(1)$ fish per cubic meter.

We have also analyzed the repeat transects from 2012 to determine group speeds for the unique aggregations that can be clearly identified in subsequent passes. These data ($N = 15$) show wide variation (an order of magnitude), with no apparent dependence on the characteristic group length scale (cube root of volume), as shown in Figure 15a. A subset of these groups was in very close proximity, making it possible to also assess their relative group speed (e.g., the speed of group A relative to the speed of group B). The observed relative speeds are approximately a factor of 2 smaller than the absolute speeds, but with similar variation (Figure 15b).

These results were presented in a special session on fish acoustics in the Spring 2014 scientific meeting of the Acoustical Society of America in Providence, R.I. A manuscript based on the final results described here is being drafted at the time of writing this report.

4. Comparing previous competing behavior models with published 3-D multi-beam data

While the above new fish behavior model was being developed (Sections 1 and 2), previous competing models were compared with published 3-D multi-beam sonar data. This helped to develop methods for comparing the statistics of static behavior properties as observed in these acoustic systems as well as provide information inferred on the dynamic behavior of the fish. These methods were incorporated into the more substantial analysis described above in Section 3. The Niwa and Anderson models were compared with 3-D multi-beam data collected by Paramo and Gerlotto. The data were consistent with the Anderson model in that both the data and model had a mode in the statistics of fish school dimensions (whereas the Niwa model does not have a mode). This suggests that the assumptions in the Anderson model on fish dynamics apply to these fish—the rate at which fish exit the school is proportional to school size. A paper was submitted describing our results: Stanton et al (submitted).

5. Echo statistics due to aggregations of fish detected by a mid-frequency long-range sonar

Reverberation was predicted for a mid-frequency long-range sonar deployed near the surface in an ocean waveguide (many km long) with schools of fish present. Two sets of calculations were made, one with the community standard PE code, and the other with a numerically efficient code that we developed. Calculations were made over a range of numbers of identical small aggregations of fish in

the waveguide. The calculations demonstrate the degree to which the statistics are non-Rayleigh, with the “tail” of the echo probability density function (PDF) increasing with decreasing numbers of aggregations (Fig. 16). Those results, as well as predictions involving a wide range of realistic waveguide conditions (including a randomized environment with internal waves), were completed and published in this paper: Jones et al. (2014).

RESULTS

We have reached major milestones of new understanding in several complementary areas: **1. Modeling of fish behavior.** The advanced modeling of fish behavior has yielded significant results. Fission, fusion, and migratory behavior of the fish have been modeled. These results use a hybrid approach that integrates both intelligence of the fish in nearest neighbor interactions as well as group behavior. Modeling of 3-D data has given information on the rate at which fish exit a school. Through use of empirical parameters and numerical optimization, realistic predictions of fish behavior have been made. **2. 3-D sonar observations of fish schools.** (a) Examination of data from several locations in the world has consistently exhibited a mode in the statistics of school dimensions, which provides information for the modeling in #1 above. (b) Time series data from repeated passes of fish has provided a rare ocean investigation of fission/fusion processes yielding critical empirical information on fish dynamics in their natural environment. For example, the speed at which groups of various sizes move, split, and recombine, is rarely observed outside of laboratory settings. These data help to bound the space/time scales at which information is passed (or remains coherent) within the school. These group-level ocean data, coupled with our laboratory data involving individual fish, are being instrumental in enabling the model (through experimental parameterization) to make realistic predictions. **3. Echo statistics from a long-range sonar in the presence of fish schools.** Predictions have demonstrated that the echoes from fish as measured by a long-range sonar are strongly non-Rayleigh over a wide range of realistic conditions. Specifically, the echo PDF’s are “heavy tailed” and the degree to which the tail of the echo distribution is non-Rayleigh depends directly upon the number of patches of fish are in the sonar beam. The level of the tail increases with decreasing numbers of aggregations.

Overall, the combination of the new modeling and measurements of fish schools, along with the predictions of echo statistics associated with long-range sonars, provides a powerful suite of tools to make realistic predictions of long-range sonar performance in the presence of fish and under a wide range of realistic conditions.

IMPACT/APPLICATIONS

The modeling and observations of fish behavior represent an advancement of the fundamental understanding of fish behavior. A key advancement in the modeling is including fish “intelligence”. Integrating the 3-D ocean data with the model is creating a powerful tool for making realistic predictions of fish behavior. The modeling of echo statistics from a mid-frequency sonar with fish aggregations present demonstrates the fish clutter characteristics relevant to Navy ASW applications. The observed speeds of fish schools yields information on the degree to which fish impact Doppler-sensitive sonars. The advanced behavior model is in a form that can be incorporated into the echo statistics model. The combination of the two models, grounded by our observations of fish behavior, provides a significant tool for predicting sonar performance associated with the presence of fish.

TRANSITIONS

The 3-D fish shoal data, provided by NOAA Fisheries and analyzed in this project, were the basis for a transition of the biologic simulations in the HiFAST FNC ONR program (LaCour, Stanton, Jones) to the CASE (NAVAIR) sonar trainer. In addition, transition of the shoal data into the SAST ACB15 (NAVSEA) sonar trainer via the HiFAST program has been approved and is currently being incorporated into the system at the time of this writing.

RELATED PROJECTS

Parts of this project fed into the concurrent ONR HIFAST FNC program (LaCour, Stanton, Jones) in which fish echoes were simulated for use in Navy sonar trainers (SAST-NAVSEA and CASE-NAVAIR) (see “Transitions” above). The 3-D multi-beam data involving fish shoals from the Eastern Bering Sea, provided by NOAA Fisheries and analyzed in this project, were used in the HiFAST program to predict echoes from shoals.

PUBLICATIONS (Refereed)

Grunbaum, D. (2012) A spatially explicit Bayesian framework for cognitive schooling behaviors. *Interface Focus*. doi: 10.1098/rsfs.2012.0027 [published, refereed]

Grünbaum, D. and M. A. Willis. (2014) Spatial memory-based behaviors for locating sources of odor plumes. *Movement Ecology*. [submitted, refereed].

Jones, B.A., J.A. Colosi, and T.K. Stanton (2014), “Echo statistics of individuals and aggregations of scatterers in the water column of a random, oceanic waveguide,” *J. Acoust. Soc. Am.*, DOI 10.1121/1.4881925 [published, refereed]

Stanton, T.K., Bhatia, S., J. Paramo, and F. Gerlotto (submitted), “Comparing modeled group size distributions to 3-D multibeam sonar data on fish school dimensions,” *Can. J. Fish. Aq. Sci.* [submitted, refereed]

Fusion-fission dynamics model for fish school behavior

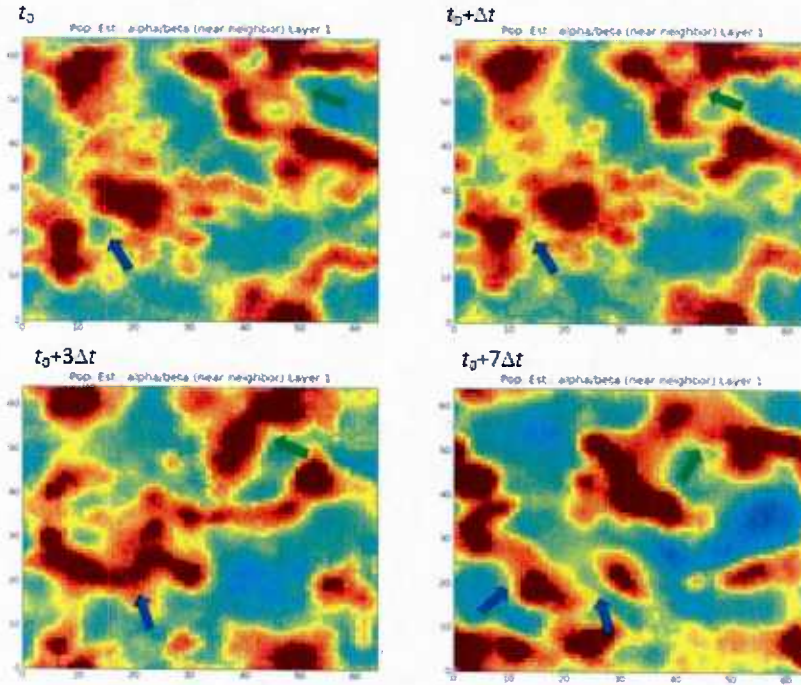


Figure 1. Fission-fusion dynamics in the cognitive schooling model, reflected in population-level density distributions at four sequential time steps (note varying time increments between images). Blue arrows indicate approach and then fusion of two groups, followed by a subsequent fission event and incipient fusion with another group. Green arrows indicate a simultaneous approach/fusion/fission sequence in a different part of the simulation domain. Computations using new model published in Grunbaum (2012).

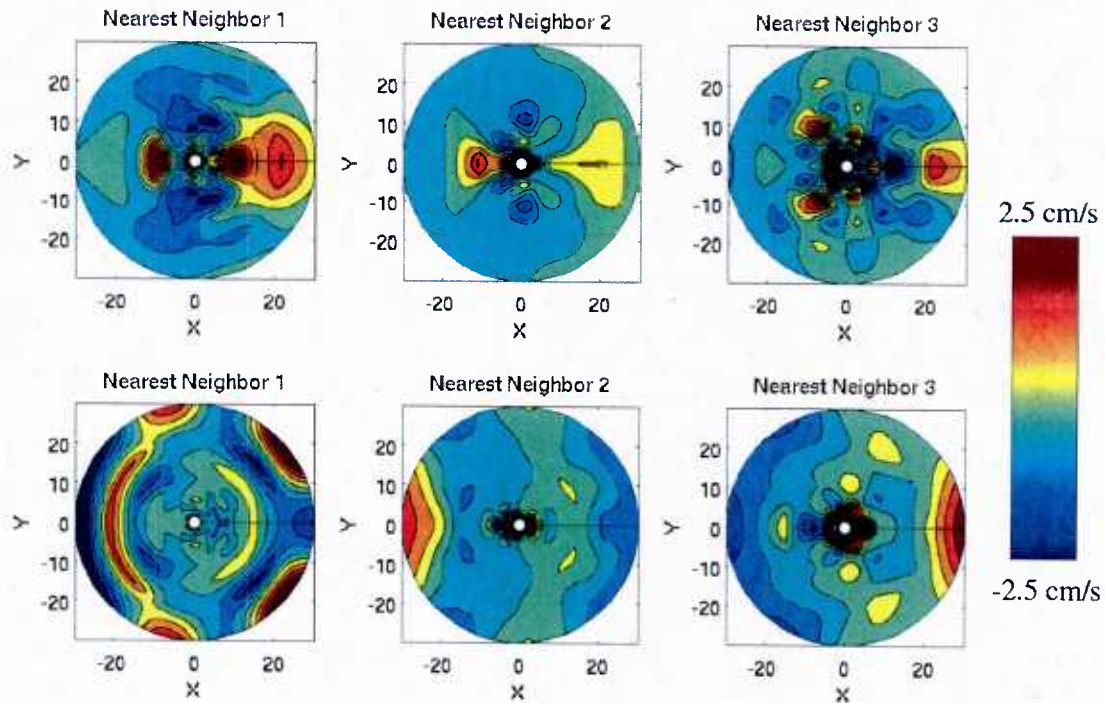


Figure 2. Numerical optimization of behavioral responses to neighbors in a diffuse milling group (top row) and a polarized group (bottom row). The graphics are “heat maps” representing speed adjustments in response to neighbors that minimize errors in predicted movements relative to 10-minute 3-dimensional trajectories of Giant Danios in the laboratory (Viscido et al. 2004, 2005, 2007). In the optimization, fish are assumed to respond to the nearest three neighbors within 30cm. Colors represent changes relative to the overall average observed swimming speed (red = +2.5 cm per sec.; blue = -2.5 cm per sec). The focal fish is at the center of each circle; movement is to the right. For example, the top left graphic shows that if a focal fish in a diffuse milling group has a nearest neighbor 20 cm ahead, its speed is predicted to increase by approximately 2.5 cm/s. The bottom left graphic shows that a focal fish in a polarized group has a nearest neighbor in the same position, its speed is predicted to decrease by approximately 1.5 cm/s.

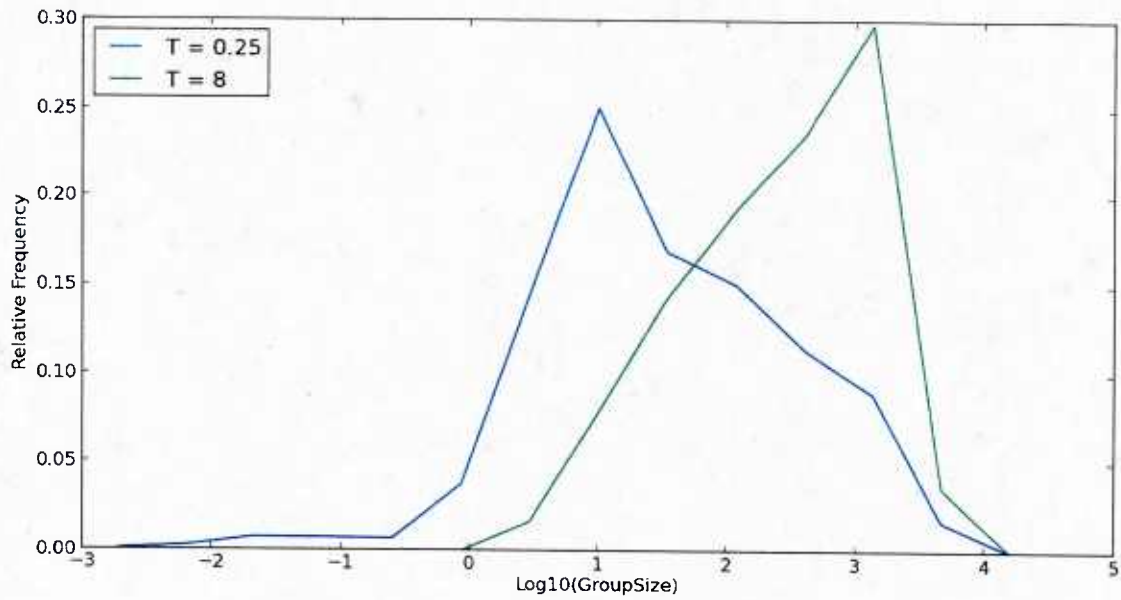


Figure 3. An example of group size distributions from school segmentation in the cognitive schooling model using mathematical morphology techniques. Size is quantified as the total number of fish within separate schools. Units are arbitrary (rescaled and nondimensionalized from physical units). This plot illustrates the strong effect of spatial memory on group- and population-level dynamics: Here, a shift from an effectively “short” memory ($T < 1$) to an effectively “long” memory ($T > 1$) results in an increase in modal group size of roughly two orders of magnitude.

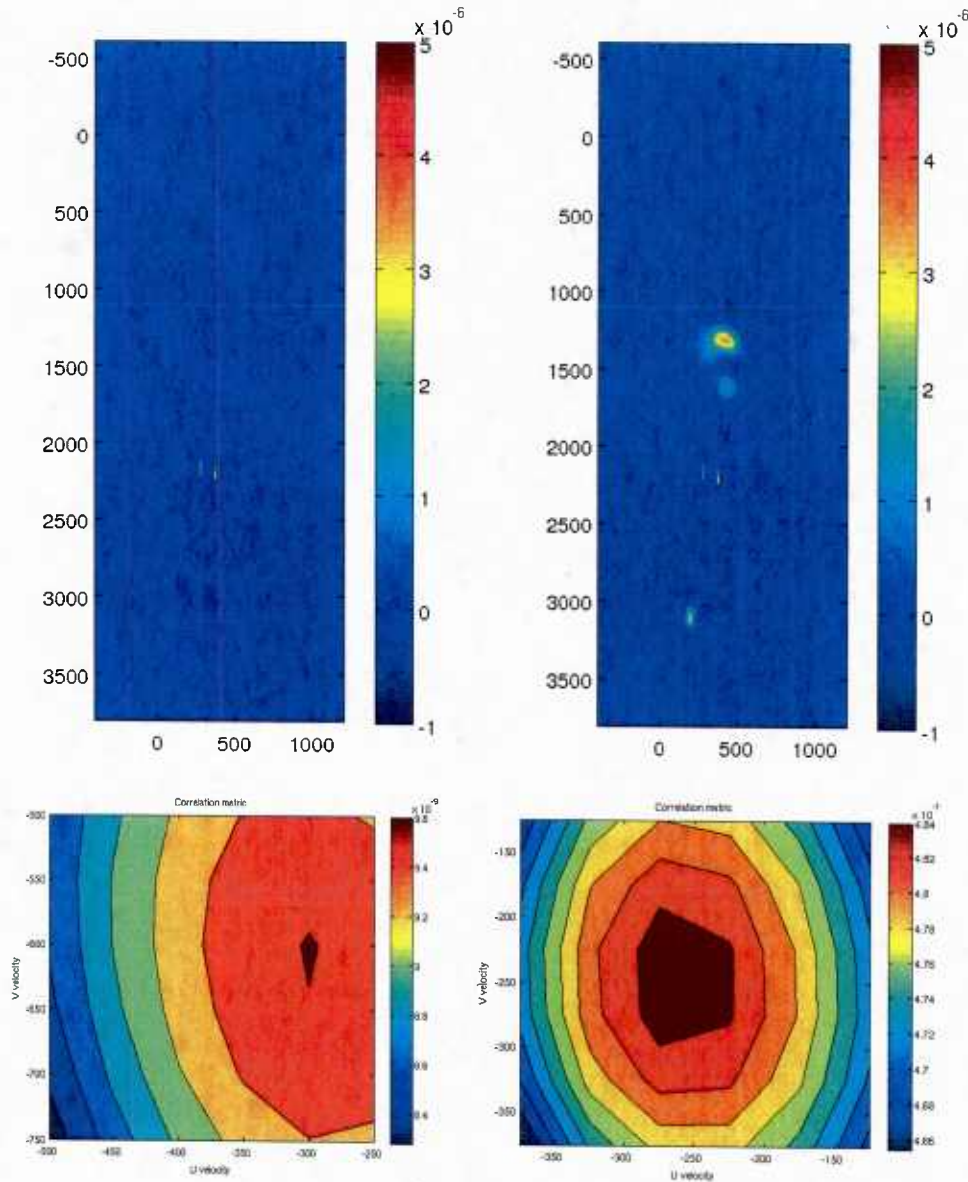


Figure 4. Numerical optimization of fish school movement parameters from NOAA Alaska Fisheries Science Center acoustic/trawl walleye pollock survey in the Gulf of Alaska. The top left graphic shows the observed acoustic backscatter from one section of a repeated survey. The top right graphic shows the simulated fish population distribution, in which location and density of fish schools are projected forward according to an advection-diffusion model. When available, predicted fish densities are replaced by observations, and subsequently carried forward by model dynamics. The bottom left graphic shows the correlation between predicted and observed fish distributions as a function of horizontal velocity in the 50m depth stratum. The strong peak in the middle right of this graphic indicates the estimated ambient current velocity, possibly with a contribution from directional movement of the fish population, within this stratum. The bottom right graphic shows the corresponding estimated velocity in the 90m depth stratum.

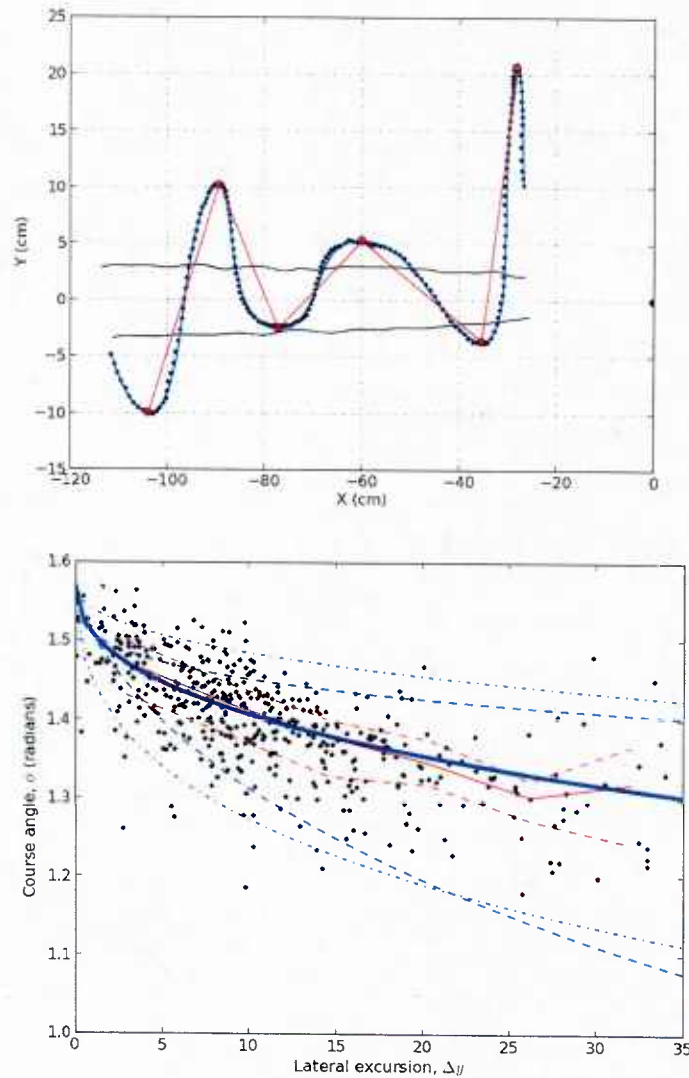


Figure 5. Development of an estimation scheme for cognitive movement behaviors using observed trajectories of a simplified behavior: location of the source of an odorant plume in a turbulent flow. The top plot shows movement of a male moth seeking a pheromone-emitting female, with the odorant source indicated by a black semicircle on the right side. Wind direction is right to left. In this plot, black circles indicate the raw position data; the blue line represents a corrected path after filtering to remove frame rate noise. The red line segments represent straight-line connections between maximum lateral excursions. The bottom plot shows the course angle and lateral excursion of 458 cross-plume transits, aggregated from four flights by each of 19 moths. The observed data are summarized by the median (solid red line) and 25th and 75th percentiles (dotted red lines). The blue solid line indicates best-fit predictions of a cognitive behavioral model ($p < 0.01$, $r^2 = 0.43$); dotted blue lines represent a sensitivity analysis for these predictions. These results indicate the methods and results being pursued to estimate fish schooling behavioral parameters from acoustic survey data. From Grünbaum and Willis (2014).

Sonar imagery of fish schools

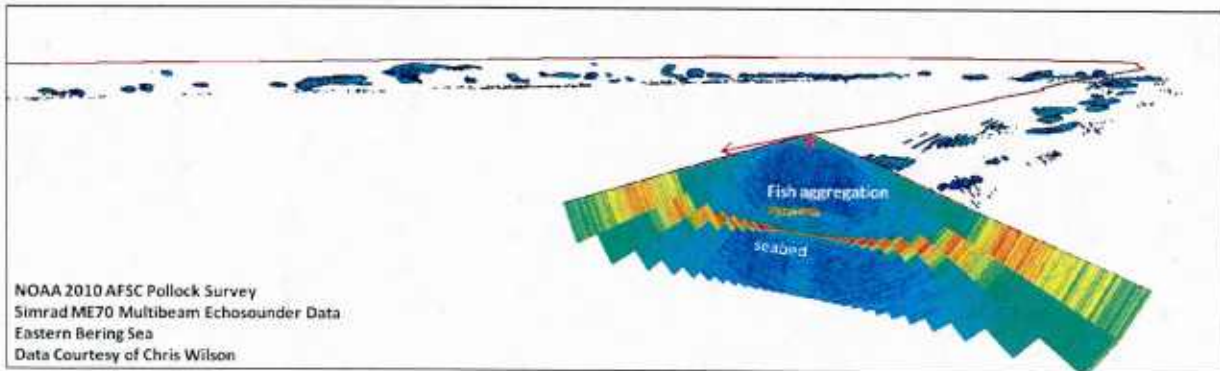


Figure 6. Example of Simrad ME70 multibeam data collected by NOAA-AFSC in the Eastern Bering Sea. A single ping of data representing a 'slice' of the water column is shown in the foreground. Target detections representing aggregations of walleye pollock are shown in the background. The ship's track line is shown in red.

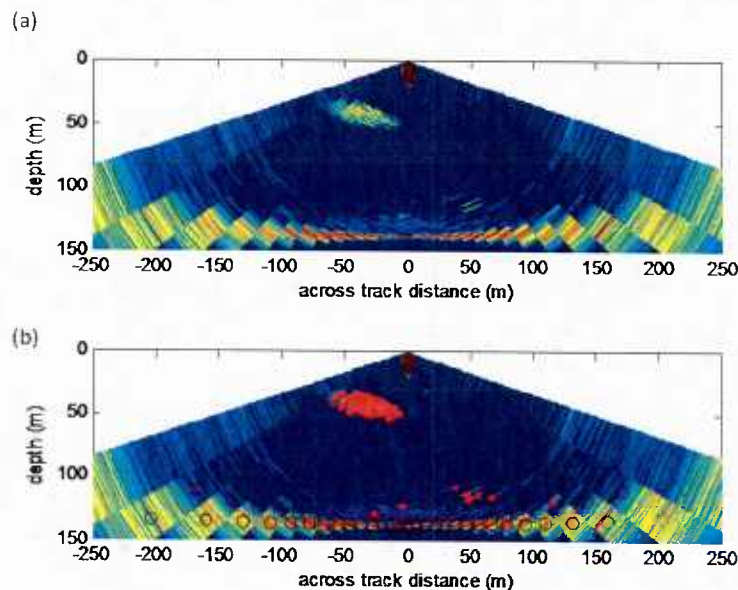


Figure 7. (a) A single raw ping of ME70 MBES data, with a small aggregation of fish located at (-40 m, 40 m). (b) Automatically detected potential fish targets (red dots) after removal of data below the seabed returns (red circles).

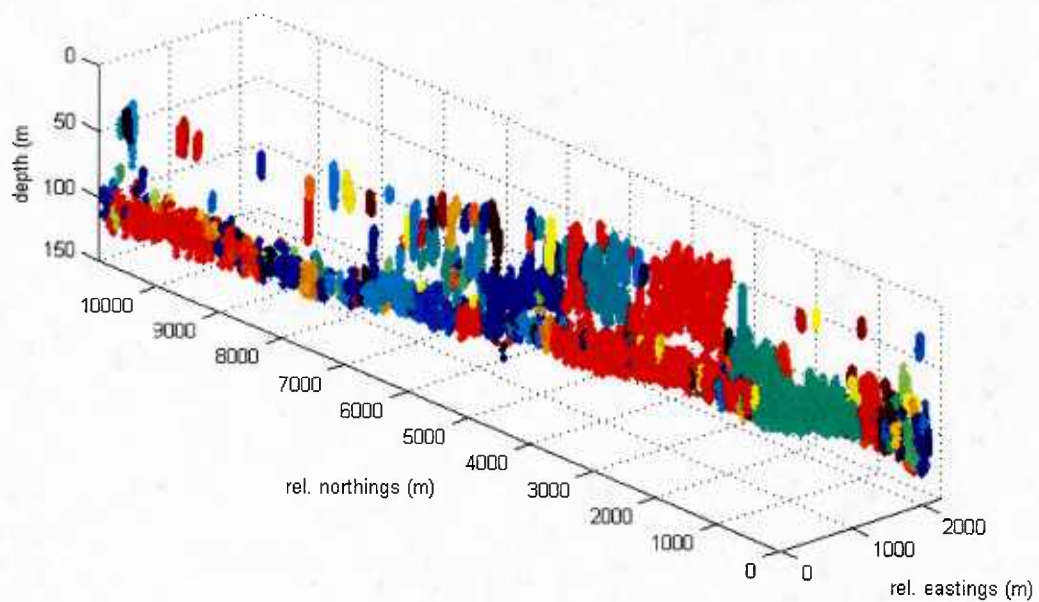


Figure 8. ME70 MBES targets classified as fish including both adult pollock (large lower layer) and smaller aggregations of juvenile Pollock (upper layer).

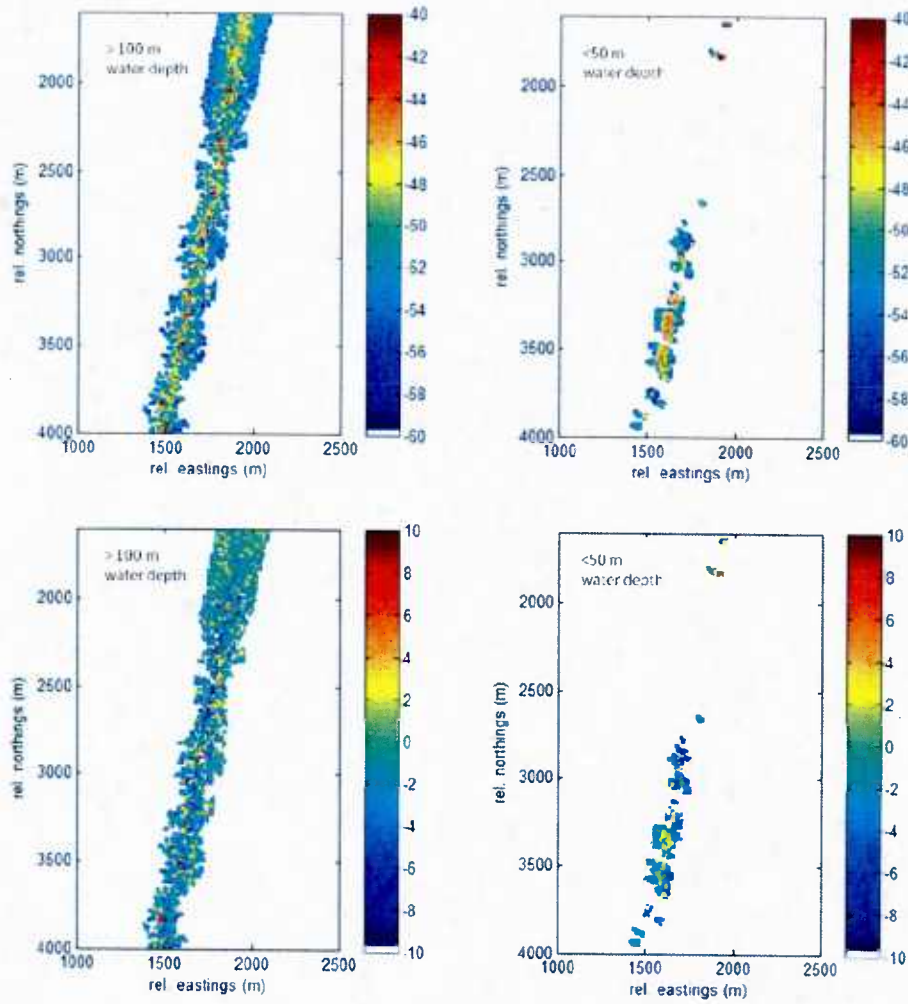


Figure 9. Upper panels: Average volume scattering strength (S_v) for the lower layer (> 100 m water depth) of adult pollock and the smaller aggregations of juvenile pollock in water depths < 50 m. Lower panels: Average S_v after normalization, which empirically removed (multi-beam) angle-dependence of scattering. This normalized scale provides a better proxy for fish number density than in the upper panels.

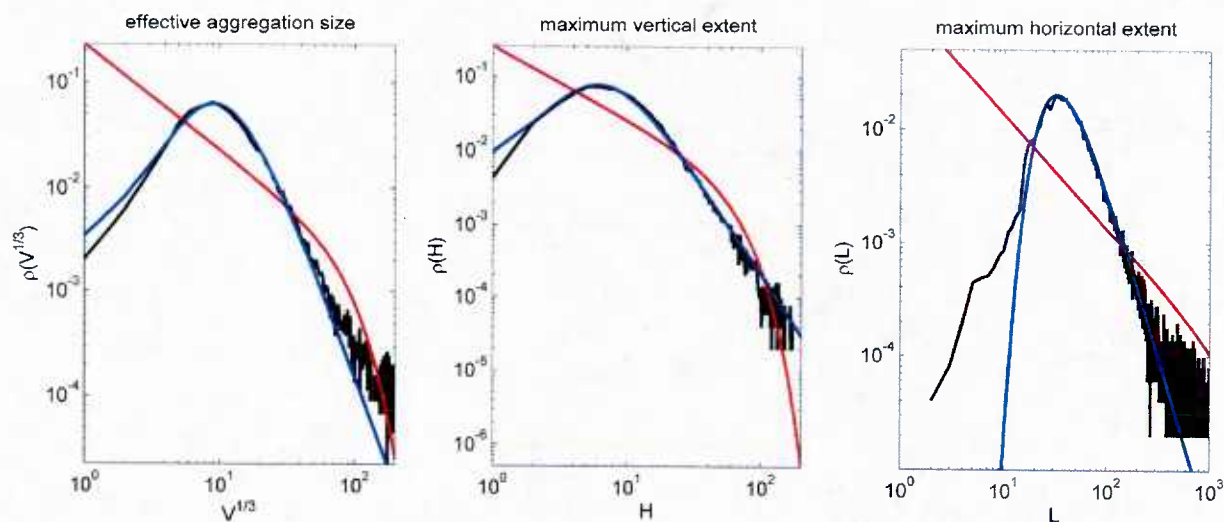


Figure 10. Statistics of fish school dimensions. Black line: Size distributions for effective size, maximum vertical extent, and maximum horizontal extent, as measured by NOAA-AFSC in the Eastern Bering Sea. Red line: Niwa's model. Blue line: Anderson's model. Note that the axes change for each plot.

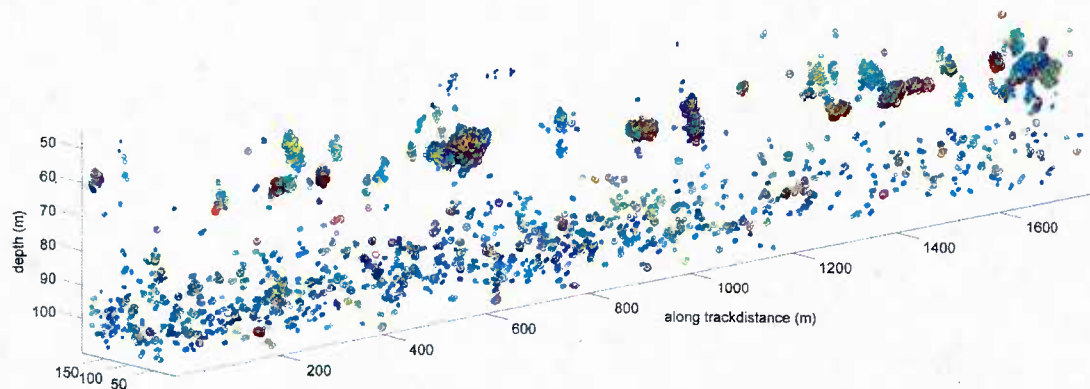


Figure 11. An example transect from the first set of repeat transects (school subset 1) in the Eastern Bering Sea, with dense aggregations of fish in the upper 80 m and a loose aggregation of fish below 80 m.

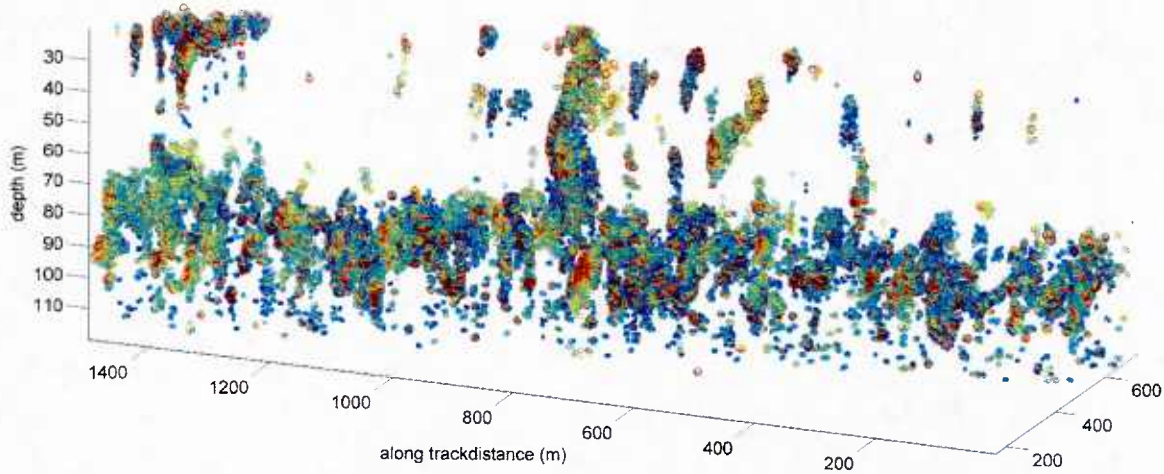


Figure 12. An example transect from the second set of repeat transects (school subset 2) in the Eastern Bering Sea, with dense aggregations of fish found throughout the water column.

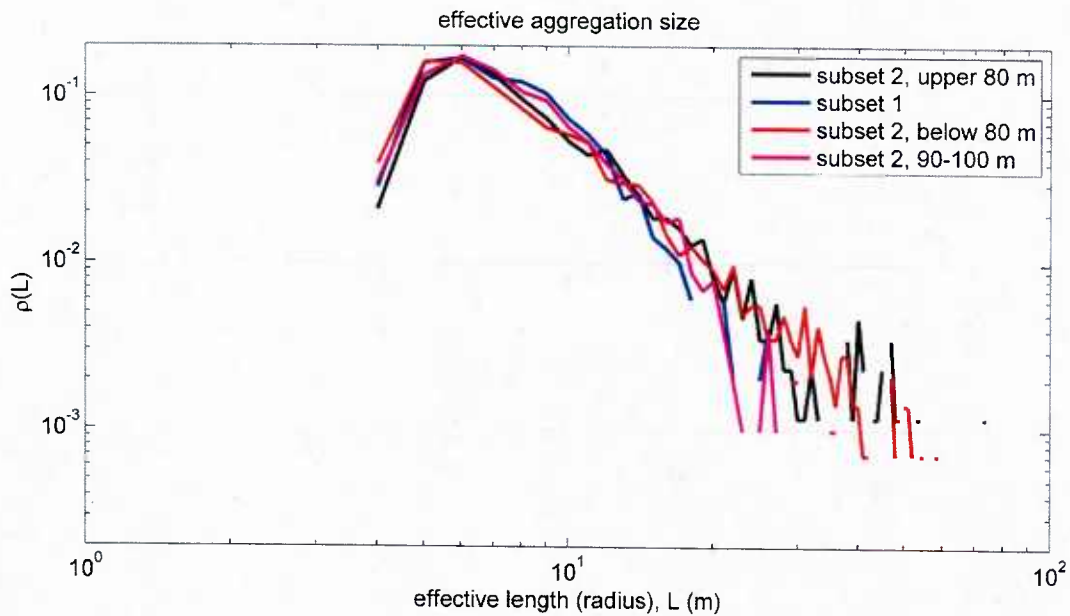


Figure 13. Distributions of effective sizes of fish aggregations (based on Fourier descriptors) were calculated for both subsets of fish data (see legend) from Eastern Bering Sea, and appear similar in all cases. For values beyond the mode, there is a power-law appearance (similar to Figure 10) in all cases, with the possible exception of subset 1.

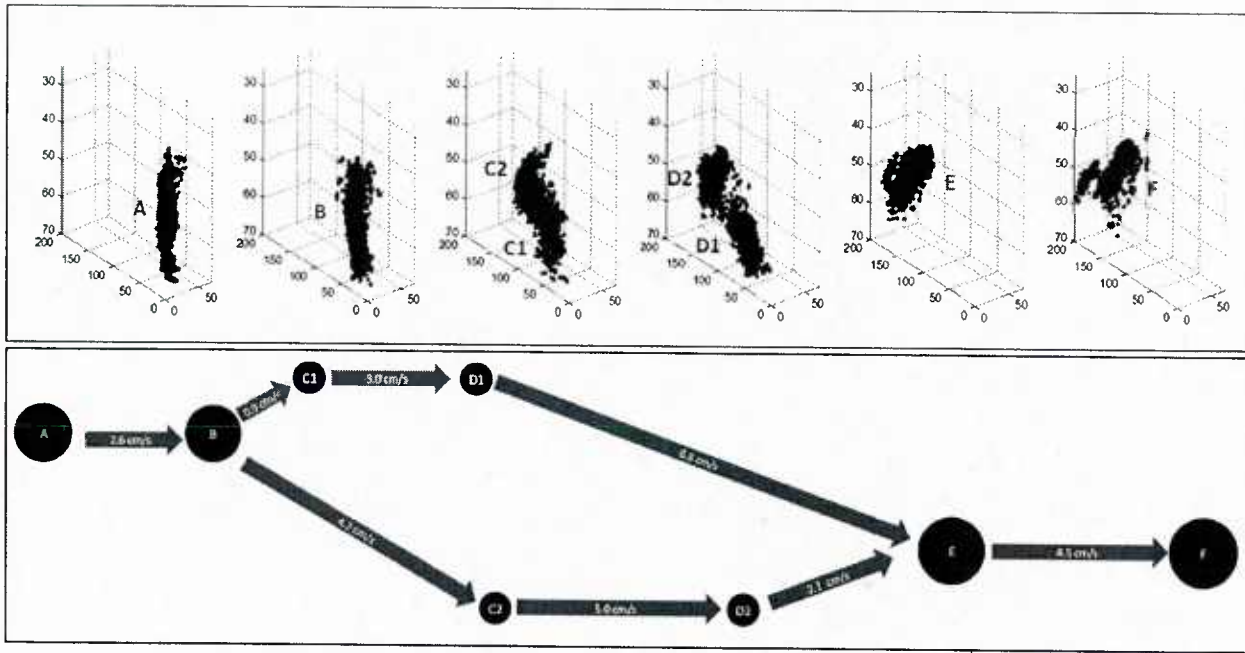


Figure 14. Anatomy of a fission (B to C1/C2) and fusion (D1/D2 to E) event. The upper panel shows raw detections extracted from six subsequent passes over an aggregation of fish with a multibeam echosounder data (5x vertical exaggeration). The lower panel describes the change in aggregation structure from pass to pass. In the lower panel, the size of the circles are proportional to the estimated number of fish, and the length of the arrows are proportional to the distance the school has moved. Data collected by the NOAA Alaska Fisheries Science Center acoustic/trawl walleye pollock survey in the Gulf of Alaska, 2012.

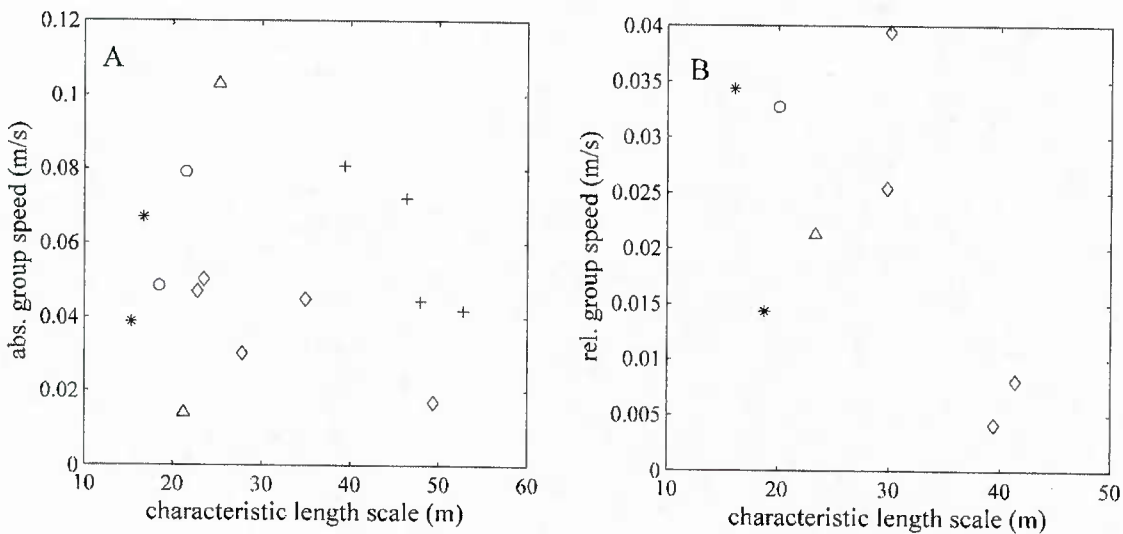


Figure 15. Absolute and relative group speeds as a function of group size observed from repeat-pass multibeam echosounder transects.

Long-range sonar: Echo statistics due to fish schools

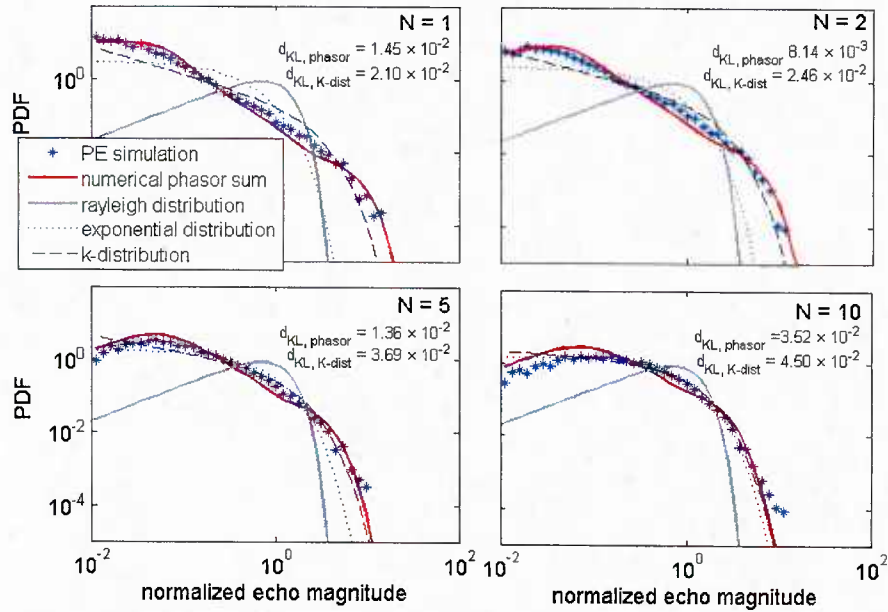


Figure 16. Modeled echo statistics from a mid-frequency sonar in an ocean waveguide with small patches of fish present. Four examples are given in which there are 1, 2, 5, and 10 identical patches present. The echo distributions are shown to be “heavy tailed” in each case. From Jones et al. (2014).